26
CO Clean-up: Water Gas Shift and Methanation Reactions

Andre C. van Veen, Yves Schuurman, and Claude Mirodatos

Analyzing topics related to the implementation of microstructured reactors for the water gas shift (WGS) and methanation reactions, there is a striking contrast between (i) a large and renewed R&D effort around both the conventional industrial processes and the development of new catalyst formulations and (ii) the scarce open literature oriented towards WGS and methanation process intensification by means of microstructured reactors. Facing that situation, we recall first the chemical background of these two reactions and process implementation, then present a brief survey/state of the art of the industrial catalysts and some new developments in catalyst formulation and finally we survey the scarce literature dedicated to microstructured reactors for these two reactions, ending with some conclusions.

26.1
Background of the Two Reactions

The WGS and the methanation reactions are well-established industrial processes implemented in large-scale hydrogen purification after steam reforming of natural gas or light hydrocarbons. High-temperature CO conversion by water gas shift (HT-WGS) is common to all hydrogen production processes given that it raises the hydrogen yield and removes simultaneously carbon monoxide. According to the desired hydrogen quality, further downstream processing involves pressure swing adsorption (PSA) for pure hydrogen production while low-temperature water gas shift (LT-WGS) followed by methanation is applied when aiming at industrial gas qualities. PSA remains a fairly bulky unit with several vessels involved in time-shifted adsorption–hydrogen release–regeneration cycles to achieve a continuous process [1]. The essential drawback of the LT-WGS followed by methanation relates to the need for carbon dioxide removal by absorption prior to the methanation, given that both carbon monoxide and dioxide can be converted, associated with hydrogen consumption. Indeed, hydrogen obtained in the latter case contains methane, but its presence is usually acceptable in most hydrogen-utilizing processes.

Micro Process Engineering, Vol. 2: Devices, Reactions and Applications.
Edited by V. Hessel, A. Renken, J.C. Schouten, and J.-I. Yoshida

ISBN: 978-3-527-31550-5

Renewed interest in these CO conversion reactions has arisen in the light of fuel cell applications. The most suitable fuel cell for small-size applications is the polymer electrolyte membrane fuel cell (PEMFC) – also called the proton exchange membrane fuel cell (PEMFC), as it supplies continuously electrical energy from fuel at high levels of efficiency and power density. It also offers the advantage of minimal maintenance given the absence of moving parts in the power-generating stacks of the fuel cell system. Temperatures are low (60–80 °C, although new development generations are progressing to operate at 100–120 °C or even higher temperatures) and the solid electrolyte minimizes problems related to corrosion. These fuel cells use hydrogen as fuel and oxygen or air as oxidant. The hydrogen can be produced from hydrocarbon fuels or alcohols by a reforming step. This typically yields a mixture of hydrogen, carbon monoxide, carbon dioxide and steam. For the reasons described below, fuel reformers also contain several units to purify the reformate mixture. To obtain good efficiency, these different units need to have well-integrated heat management. In this respect, microstructured reactors are beneficial for these applications. Figure 26.1 shows an example of a microstructured based 5 kW fuel processor for isooctane that has been reported [2, 3].

At these low PEMFC operating temperatures, the only active anode catalyst material is platinum. Unfortunately, carbon monoxide chemisorbs more strongly than hydrogen on platinum and even small CO concentrations lead to a substantially lower energy output of the fuel cell. Therefore, any fuel processor producing hydrogen from hydrocarbons or alcohols needs to provide a section after the reformer lowering the CO concentration in the reformate to approximately 50 ppm, depending on the fuel cell characteristics (i.e. levels might be raised to 100–500 ppm for the new PEMFC generations).

The CO clean-up section typically consists of different units, usually a one- or two-stage WGS reactor, followed by a unit to remove the final traces of CO such as a selective oxidation (SELOX) – also called preferential oxidation (PrOx) unit, a methanation unit or a physical separation method (Pd–Ag-based membrane, PSA). It would often be desirable to eliminate the LT-WGS unit, as it constitutes a rather large-sized and heavy unit. However, heat management restrictions and the still rather low efficiency of the PrOx unit require low CO concentrations in the feed. On the other hand, methanation would become more attractive once an enhanced selectivity permits conversion of CO without conversion of CO_2, as this then no longer requires upstream CO_2 separation.

For feeds containing relatively high concentrations of CO, the WGS reaction can effectively convert CO into CO_2 by reaction with water over a suitable catalyst:

$$\mathrm{CO + H_2O = CO_2 + H_2} \quad \Delta H^{\emptyset} = -41.1\ \mathrm{kJ\ mol^{-1}}, \quad \Delta G^{\emptyset} = -28.6\ \mathrm{kJ\ mol^{-1}} \tag{26.1}$$

This reaction produces additional hydrogen and increases the overall process efficiency. The reaction is exothermic and low reaction temperatures push the thermodynamic equilibrium towards high CO conversions. However, fast kinetics are only obtained at high temperatures. The need to speed up the reaction rate has resulted in the use of two (or more) WGS reactors in industrial applications. Generally, low-temperature (LT) and high-temperature (HT) operations are used,

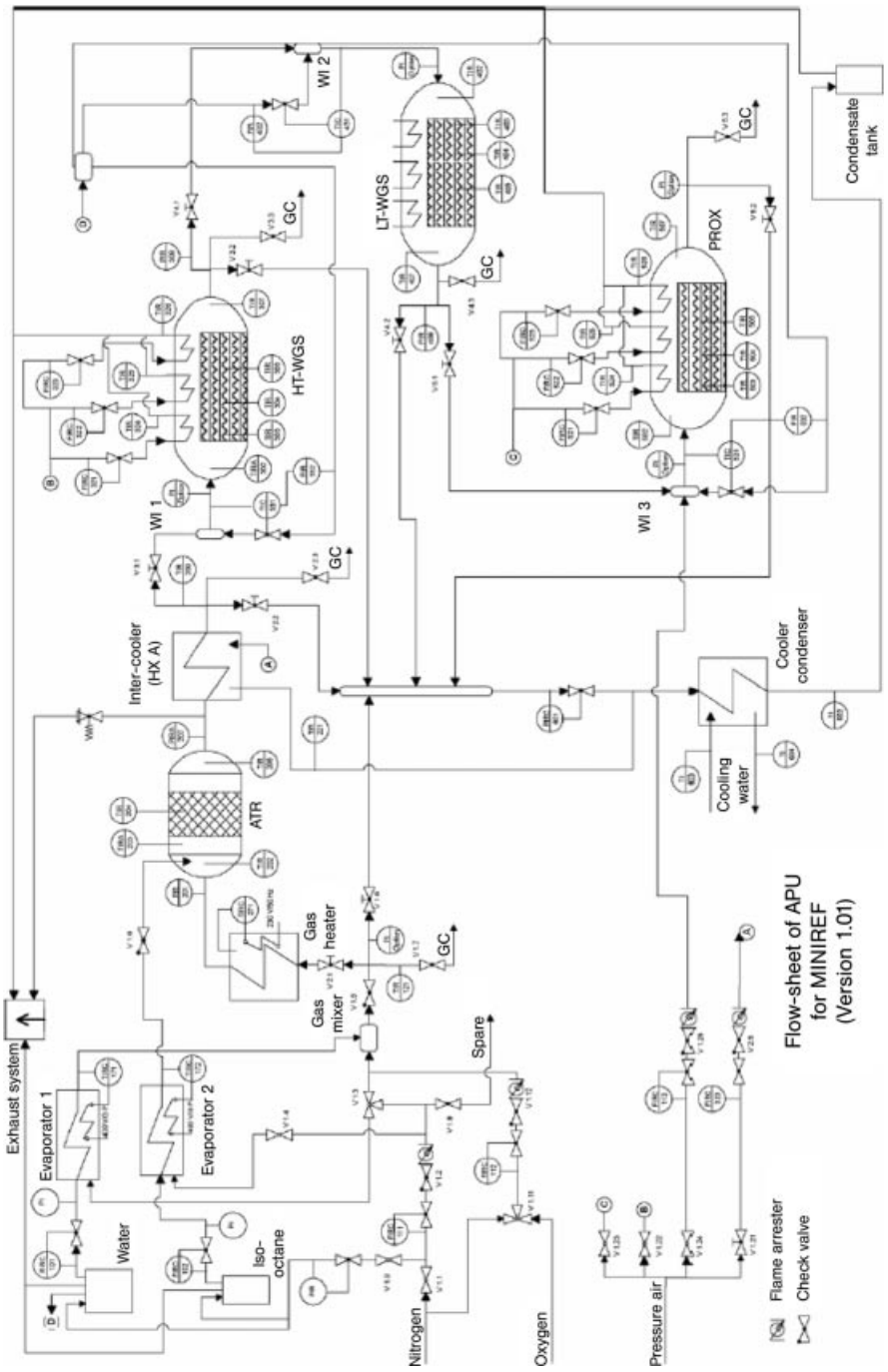

Figure 26.1 Flow scheme of a fuel processor, comprising microstructured reactors [3].

with inter-bed cooling and with different catalysts for the different stages. In this way, the CO concentration can be reduced to <0.3%. As shown above, after the single- or double-stage shift, the CO content has to be lowered further to about 50 ppm by either methanation of CO into methane or by preferential oxidation of CO into CO_2, with both reactions taking place over an appropriate catalyst.

26.2 Commercial and R&D Catalysts

Commercial catalysts used for HT shift are based on iron oxides and are used in the temperature range 320–450 °C [4]. A typical catalyst will consist of 80–90% Fe_2O_3 and 10–20% Cr_2O_3, sometimes with other additives. They are manufactured using a coprecipitation method. The iron oxide WGS catalyst requires careful reduction before use. Catalyst pretreatment involves the partial reduction of hematite to magnetite (of Fe_2O_3 to Fe_3O_4) using process gas mixtures of hydrogen, nitrogen, carbon monoxide, carbon dioxide and water vapor, and formation changes can take up to 2 weeks to complete. These catalysts are very stable and can have a lifetime of many years. Deactivation is usually attributed to a loss of active surface area and catalyst poisoning, mainly by sulfur. Polymerization of hydrocarbons can block pores and there are also reports of phosphorus and silicon compounds acting as poisons. In industrial reactors, problems occur due to pore diffusion limitations when operating at higher temperatures.

Commercial catalysts used for LT shift are based on copper and zinc oxide and are typically operated in the range 180–250 °C [4]. Typical commercial catalysts consist of approximately 30% CuO, 30–50% ZnO and 15–30% Al_2O_3. The influence of many different additives has also been investigated. Preparation generally involves coprecipitation. The reduction of the copper-based shift catalyst is normally carried out using a diluted dry hydrogen stream (ca. 3% H_2/N_2). Care must be taken during reduction, which, due to the exothermic reaction, may result in excessive catalyst temperatures and severe sintering of the active phase: LT shift catalysts are notoriously sensitive to deactivation. This deactivation is usually coupled with the sintering of copper particles, along with poisoning by sulfur, chlorine and silica.

A third kind of shift catalyst is commercially available, specifically aiming at those applications having a sulfurous gas stream. The catalyst is based on a mixed cobalt/molybdenum oxide. The catalyst needs sulfidation before it becomes active. The gas phase needs to contain a minimum amount of H_2S or COS to keep the catalyst in its active sulfide form.

New generations of catalysts still at the R&D stage combine reducible supports such as (doped) ceria and magnesia supporting noble and non-noble metals [5–19].

26.2.1 Temperature Range of Operation

Most HT-WGS reactors operate at about 300–350 °C inlet temperature and lower the CO level from 10–15 mol% (dry) to 1–2 mol% (dry). The LT-WGS reactor operates at

about 190–210 °C inlet temperature and lowers the CO level from 1–2 mol% (dry) to 0.1–0.2 mol% (dry). Ideally, the catalysts take the reaction to equilibrium at the lowest temperature possible to favor hydrogen production and carbon monoxide conversion.

It is important to note that conventional HT-WGS catalysts are inactive below 300 °C, whereas conventional LT-WGS catalysts degrade above 250 °C.

26.2.2
Operational Limits

In general, several severe requirements are imposed by the composition and structure of the WGS catalysts under industrial conditions. For instance, the iron-based HT-WGS and copper-based LT-WGS catalysts have the following operational limits:

- Since both catalysts burn up when exposed to air (pyrophoric), they must be sequestered during system shut-down when only air flows through the system.
- The inlet gas temperature must be above the dew-point with a reasonable margin as water condensation damages the catalyst. This limits the minimum inlet temperature to around 190 °C for the LT-WGS system at atmospheric pressure.
- The LT-WGS catalyst is affected by traces of poisons such as sulfur and chloride (if present), which have little effect on and pass through the upstream reforming and HT-WGS section at sub-ppm levels.
- Byproduct, i.e. methanol (and amine) production over LTS catalysts is a concern for both environmental and efficiency reasons. This is partly solved by the addition of K_2O and Cs_2O modifiers.

26.2.3
Non-pyrophoric Catalysts

As seen above, the two commercial shift catalysts are highly pyrophoric. Exposure to air of the $Cu/ZnO/Al_2O_3$ and the FeCr catalysts results in "theoretical" temperature rises of about 800 and 450 °C, respectively (in DTA experiments). Although under industrial conditions this problem is dealt with by special passivation and reduction procedures, this might not be feasible for smaller fuel processors. In addition to high activity, other requirements have to be fulfilled for PEM applications: fast response, long lifetime and non-pyrophoric materials.

Several new non-pyrophoric WGS catalysts have been reported in the literature, such as Au/Fe_2O_3 [6, 7], Au/CeO_2 [7, 8], Au/TiO_2 [9], Ru/ZrO_2 [10], Rh/CeO_2 [11] Pt/CeO_2 [7, 12, 13], Pt/ZrO_2 [14], Pt/TiO_2 [15], Pt/Fe_2O_3 [16] and Pd/CeO_2 [17], as promising catalysts for fuel cell applications as they are less sensitive to air exposure than the industrial types. These catalyst formulations typically consist of a precious metal (Pt, Rh, Ru, Pd, Au) deposited on a (partially) reducible support (CeO_2, TiO_2, ZrO_2). Some non-noble metal-based catalysts have also been reported: Cu/CeO_2 [18, 19], Ag/TiO_2 [9], Cu/TiO_2 [9] and Cu/ZrO_2 [20]. Grenoble *et al.* [21] and Panagiotopoulou and Kondarides [22] showed that these catalysts are bifunctional, i.e. both the metal and support have a significant influence on the overall performance.

The activity of these non-pyrophoric catalysts is between those of a commercial Cu/Zn/Al_2O_3 catalyst and a commercial Fe/Cr, thus working at intermediate temperatures, 250–400 °C.

26.2.4
Methanation Catalysts

Commercial methanation catalysts are supported nickel systems and have the major drawback of their sensitivity to poisons such sulfur. Another concern is the selectivity of CO methanation over that of CO_2.

New methanation catalysts with improved CO selectivity, mainly based on doped Ni oxides, were reported by Krämer *et al.* [23].

26.3
Motivation for Microstructured Reactors

Among the main usual reasons for implementing microstructured reactors, improved heat management and control of residence time distributions are considered for fast and highly exo- or endothermic reactions.

26.3.1
WGS Reaction

This reaction is moderately exothermic and the reaction rates are not very high. Therefore, the principal motivation to perform the WGS reaction in a microstructured reactor rather than in a fixed-bed reactor is that it will be part of an integrated fuel reformer. To achieve high efficiency in a fuel reformer, the different endothermic and exothermic steps need to be combined. Microstructured fuel reformers can reach a high degree of integration within a small volume. The usually bulky WGS reactors would benefit greatly from a reduction in the catalytic volume. Microstructured reactors would present such an advantage for the WGS reaction. As the reaction is reversible and exothermic, performing the reaction with a forced optimal temperature profile will lead to smaller reactor volumes compared with adiabatic operation.

26.3.2
Methanation Reaction

Being a very strongly exothermic reaction, the main interest in the use of microstructured reactors for the CO methanation reaction is the excellent heat management in order to control the reaction temperature. Given that the suppression of upstream CO_2 removal is imposed by a compact system design, methanation units would handle feeds containing both CO and CO_2, thus imposing a conversion selectivity challenge. Generally, the conversion selectivity of CO against CO_2 drops with increase in temperature, causing additional loss of hydrogen and higher energy

release. On the other hand, the need to decrease the unit sizes imposes operation of the methanation at reasonably elevated temperatures to attain high reaction rates. Using a conventional reactor could potentially lead to a loss of process control and runaway of the reactor, while a microstructured device would remain in control.

26.4
Examples of Microstructured Reactor Developments

Very few literature reports exist on the preparation of microstructured reactors for coating adapted catalysts and performance testing for either WGS or CO methanation reactions.

26.4.1
WGS Reaction

Germani *et al.* [24] illustrated the possible negative impact of organic binders and acetic acid used in preparing the slurry coatings on the activity of a commercial CuO/Cr_2O_3/Al_2O_3 catalyst for the WGS reaction in a MSR. Figure 26.2 shows microstructured coatings of commercial CuZnAl catalysts using two different organic binders. It can be seen (Figure 26.2, right) that the use of Tylose as binder leads to the best quality washcoat, with an approximately uniform thickness of about 30 μm. The washcoat covers the whole channel perimeter and it is compact except for some longitudinal cracks. The washcoat prepared with the poly(vinyl alcohol) binder (Figure 26.2, left), on the other hand, does not cover the whole channel perimeter and is thicker at the bottom. It can be seen that it is also less compact, confirming the results of lower bulk density and higher macroporosity. It was concluded that dissolution–complexation–redeposition processes of the metal phases especially caused by the acetic acid decreased the catalytic performance substantially.

The advantage of thin catalyst layers has been demonstrated for the WGS reaction over a Pt/CeO_2/Al_2O_3 catalyst [25]. The conversion of CO was measured at various

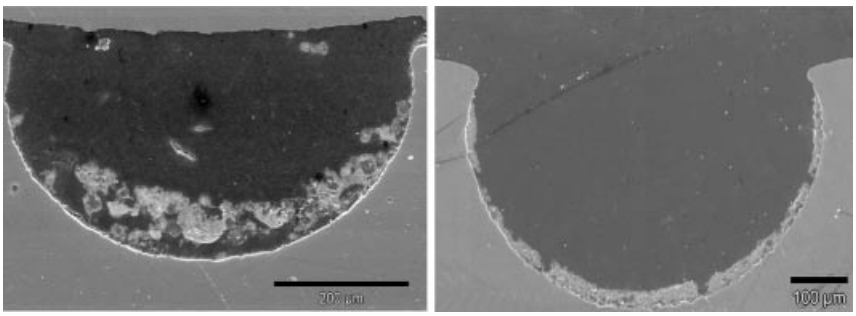

Figure 26.2 CuZnAl catalyst washcoatings prepared with a poly(vinyl alcohol) binder (left micrograph) and a Tylose binder (right micrograph).

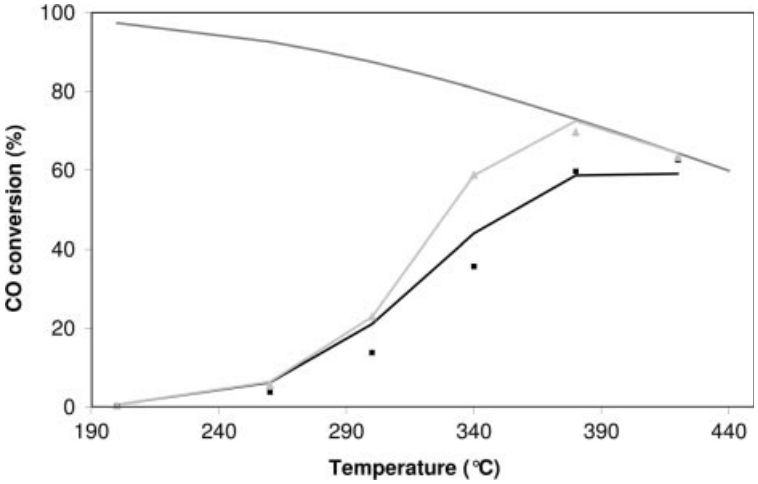

Figure 26.3 Comparison between rate of CO conversion under WGS conditions for fixed-bed (black) and microreactor (gray) both containing 250 mg of $Pt/CeO_2/Al_2O_3$. Flow rate, 200 mL min^{-1}; feed composition 32.2% H_2, 9.6% CO, 8.4% CO_2, 23.0% H_2O, 26.8% Ar [25].

temperatures over both a powder sample with an average particle size of 250 μm and over the same catalyst prepared by a sol–gel method in stainless-steel microchannels. The equivalent particle diameter of the catalyst layer inside the microchannel was 37 μm. The initial rates obtained at low temperatures over the powder sample compared well with those obtained over the microstructured platelets. However, the data deviated substantially at higher temperatures between powder and platelets, as presented in Figure 26.3. The conversion over the powder samples was lower than that of platelets, indicating that there might be a diffusion limitation inside the powder grains. A simulation that took into account the diffusion of the reactants and products inside the pores confirmed this. This kinetic study was extended and a detailed mechanism for the WGS reaction over a $Pt/CeO_2/Al_2O_3$ catalyst was derived [26], emphasizing the unique features of MSRs for intrinsic kinetic studies. An open housing was used that allowed the number of microstructured platelets to be changed between 1 and 6, as shown in Figure 26.4.

By using integrated heat exchangers, researchers at PNNL [27] were able to control the temperature of a microstructured WGS reactor and impose a near-optimal temperature profile, rather than operating the reactor as two sequential adiabatic units (Figure 26.5). The first section of the reactor, operated adiabatically, consisted of increasing the reactor temperature, while the second section was cooled to follow as closely as possible the optimal temperature profile. This way of operating the reactor resulted in a reduction in the reactor size by a factor of 2. If the reaction rate is expressed in the form of a power law:

$$r_{CO} = A^{\circ}\exp\left(\frac{-E_{act}}{RT}\right) P_{CO}{}^{\alpha} P_{H_2O}{}^{\beta} P_{H_2}{}^{\gamma} P_{CO_2}{}^{\delta} \left(1 - \frac{P_{H_2} P_{CO_2}}{K_{eq} P_{CO} P_{H_2O}}\right) \qquad (26.2)$$

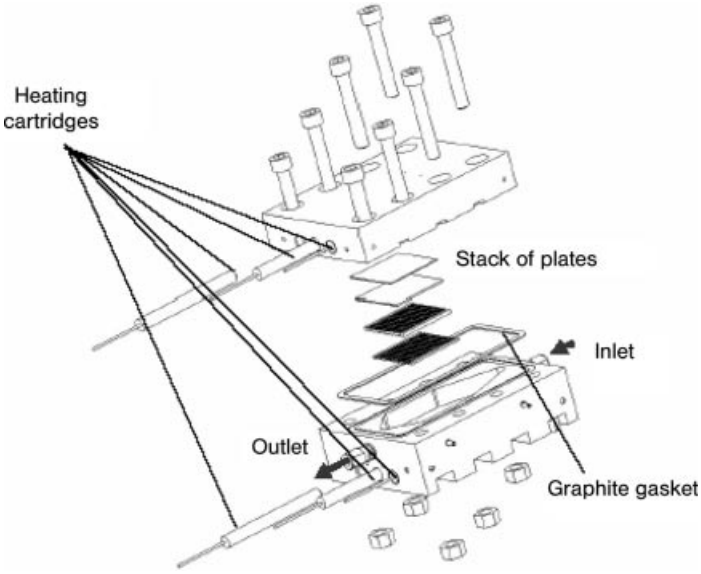

Figure 26.4 Test reactor used for the kinetic analysis of the WGS reaction over microstructured $Pt/CeO_2/Al_2O_3$ [26].

the optimal temperature is given by [28]

$$T_{\text{opt}} = \frac{\Delta H_{\text{R}}}{\Delta S_{\text{R}} - R\ln\left[\left(1-\frac{\Delta H_{\text{R}}}{E_{\text{act}}}\right)\frac{(\gamma'_{\text{H}_2}-X_{\text{CO}})(\gamma'_{\text{CO}_2}-X_{\text{CO}})}{(1-X_{\text{CO}})(\gamma'_{\text{H}_2\text{O}}-X_{\text{CO}})}\right]} \tag{26.3}$$

where γ'_j is the mole fraction of component j at the reactor inlet with respect to the mole fraction of CO. Note that the only kinetic parameter in this equation is the activation energy.

Figure 26.5 2 kW WGS microreactor with incorporated heat exchanger [27].

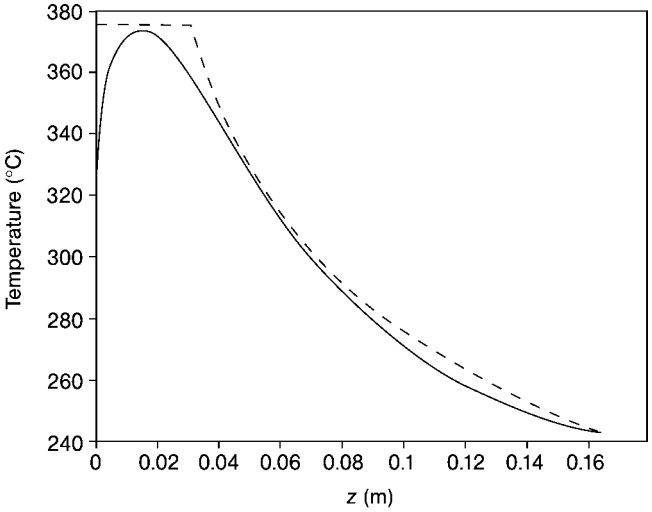

Figure 26.6 Simulated temperature profile in the reaction channel (solid line) compared with the optimum profile (dashed line) [29].

Baier and Kolb [29] investigated further the design of a countercurrent cooled microstructured reactor to establish an optimal temperature profile. Figure 26.6 shows their simulations of the temperature profile in the microstructured device compared with the optimal temperature profile. Using extensive simulations, they were able to optimize a single-stage WGS reactor that gives similar performances to the two-stage adiabatic reactor configuration. Furthermore, this microstructured unit leads to an increase in the overall energy efficiency of a reformer unit due to the smaller amount of water that is injected in the WGS unit.

Görke *et al.* [30] prepared different microstructured catalysts (Au/CeO_2 and Ru/ZrO_2) on both FeCr alloy and stainless-steel platelets for the WGS and SELOX reactions. The adhesion of the Ru/ZrO_2 catalysts was good, but the CeO_2-based catalysts did not adhere as well. The Ru/ZrO_2 catalysts on FeCr alloy platelets showed the highest activity. The authors attributed traces of chromium found on the Ru/ZrO_2 supported on stainless steel to the lower activity of this catalyst, stressing the importance of metallurgical phenomena in MSRs.

Rebrov *et al.* [31] investigated a different WGS catalyst to those mentioned above. They compared the activity and stability of two types of molybdenum carbide coatings deposited on molybdenum substrates (Mo_2C/Mo) for the WGS reaction at 513–631 K. The activity of the Mo_2C/Mo coatings obtained by molten salt synthesis in a melt containing 5 wt.% Li_2CO_3 in an equimolar NaCl–KCl mixture at 850 °C for 7 h was stable for more than 500 h on-stream at 631 K in a mixture containing 0.5 vol.% CO, 1.5 vol.% H_2O and 40 vol.% H_2 balanced by helium. There was no evidence of methanation activity on both Mo_2C/Mo coatings below 350 °C. It was shown that if molybdenum carbide is present as a thin layer over a molybdenum substrate (Mo_2C/Mo), the catalytic activity is enhanced compared with that of the pure Mo_2C phase. The

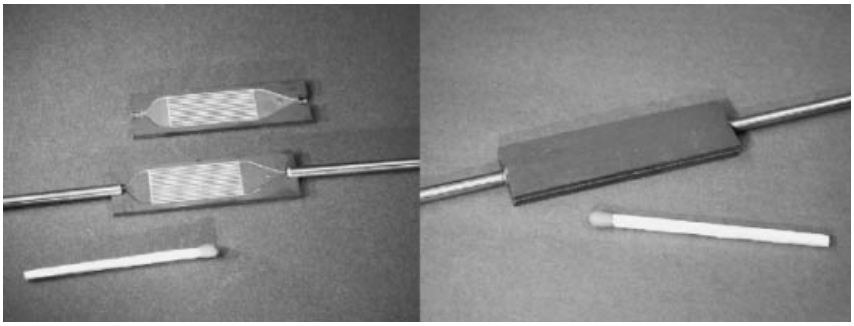

Figure 26.7 Reactor applied for screening of WGS catalysts: left, coated platelets with tubing; right, platelets attached face-to-face and sealed by laser welding. [33].

kinetics of the WGS and reverse WGS reactions were measured on Mo_2C/Mo coatings obtained by molten salt synthesis in a microstructured reactor operating in a differential mode.

Pawlak *et al.* [32] compared washcoatings of commercial catalysts and a Pt/CeO_2 sample in terms of the coating properties and catalytic performance. Unfortunately, no details of the catalysts composition were given, making the results not very useful.

Kolb *et al.* [33] tested washcoated alumina catalysts inside microchannels for the WGS reaction, in the device shown in Figure 26.7. $Pt/CeO_2/Al_2O_3$, $Pt/Rh/CeO_2/Al_2O_3$, $Pt/Pd/CeO_2/Al_2O_3$ and $Pt/Ru/Al_2O_3$ catalysts were screened at high (9%) and low (2.6%) partial pressures of carbon dioxide at 290, 315 and 340 °C. Methane was formed as the only byproduct. $Pt/CeO_2/Al_2O_3$ was identified as the best candidate with respect to selectivity and activity. The calcination temperature and platinum metal salt solution applied during catalyst preparation had a drastic effect on the activity of the $Pt/CeO_2/Al_2O_3$ catalyst. The authors mention no specific advantages of screening washcoated catalysts rather than powder samples.

26.4.2
Methanation Reaction

Selective methanation of CO has been investigated over washcoated supported metal catalysts in a microchannel reactor with simulated reformate feeding [34]. Several Ru- and Ni-supported catalysts were investigated. A $Ni/CaO/Al_2O_3$ catalyst exhibited the highest methanation activity at 300 °C with a CO conversion of more than 93% and a relatively low conversion of CO_2 into methane. Below 250 °C, CO methanation occurred exclusively. The presence of steam had an inhibiting effect on the methanation rate. Addition of oxygen suppressed the methanation activity of the catalyst and led to significant hydrogen oxidation.

Görke *et al.* [35] performed CO methanation over Ru/SiO_2 and Ru/Al_2O_3 catalysts with co-feeding of oxygen. If CO in the presence CO_2 has to be converted by methanation, a sufficient amount of O_2 has to be added and the temperature has

to be controlled precisely. The authors stated that this is easily feasible using microstructured reaction technology.

26.5 Conclusion

The use of microstructured devices for the WGS reaction is mainly motivated by system integration aspects and less by constraints imposed from catalysis. At the limit, the principal challenge for the WGS unit remains the development of more active catalysts and coating techniques attaining the highest catalyst loading of microstructured devices. Assuming that no separation units may be used in small-scale or mobile units implies that hydrogen-rich gases that enter the final purification unit will contain CO and CO_2 mixtures. In the case of methanation, selectivity of CO against CO_2 conversion is the main challenge, especially at high reaction rates and thus high temperatures. Obviously, novel catalysts with intrinsically higher selectivity could lead to significant improvements, but the excellent temperature control of microstructured devices remains a striking advantage for this reaction.

References

1 K. Knaebel, D. Ruthven, J. L. Humphrey, R. Carr, in *Emerging Separation and Separative Reaction Technologies for Process waste Reduction – Adsorptive and Membrane Systems* (eds P. P. Radecki, J. C. Crittenden, D. R. Shonnard, J. L. Bulloch), AiChe – Center for Waste Reduction Technologies, **1999**.

2 G. Kolb, T. Baier, J. Schürer, D. Tiemann, A. Ziogas, H. Ehwald, P. Alphonse, *Chem. Eng. J.* **2008**, *137*, 653.

3 G. Kolb, T. Baier, J. Schürer, D. Tiemann, A. Ziogas, S. Specchia, C. Galletti, G. Germani, Y. Schuurman, *Chem. Eng. J.* **2008**, *138*, 474.

4 C. N. Satterfield, *Heterogeneous Catalysis in Industrial Practice*, Robert E. Krieger Publishing, Malabar, FL, **1996**.

5 R. J. Farrauto, Y. Liu, W. Ruettinger, O. Ilinich, L. Shore, T. Giroux, *Catal. Rev.* **2007**, *49*, 141.

6 D. Andreeva, V. Idakiev, T. Tabakova, A. Andreeva, *J. Catal.* **1996**, *158*, 354.

7 A. Luengnaruemitchai, S. Osuwan, E. Gulari, *Catal. Commun.* **2003**, *4*, 215.

8 D. Andreeva, V. Idakiev, T. Tabakova, L. Ilieva, P. Falaras, A. Bourlinos, A. Travlos, *Catal. Today* **2002**, *72*, 51.

9 F. Boccuzzi, A. Chiorino, M. Manzoli, D. Andreeva, T. Tabakova, L. Ilievab, V. Iadakiev, *Catal. Today* **2002**, *75*, 169.

10 O. Goerke, P. Pfeifer, K. Schubert, *Appl. Catal. A* **2004**, *263*, 11.

11 T. Shido, Y. Iwasawa, *J. Catal.* **1993**, *141*, 71.

12 P. Panagiotopoulou, J. Papavasiliou, G. Avgouropoulos, T. Ioannides, D. I. Kondarides, *Chem. Eng. J.* **2007**, *134*, 16.

13 A. Goguet, F. C. Meunier, J. P. Breen, R. Burch, M. I. Petch, A. Faur Ghenciu, *J. Catal.* **2004**, *226*, 382.

14 E. Xue, M. O'Keeffe, J. R. H. Ross, *Catal. Today* **1996**, *30*, 107.

15 P. Panagiotopoulou, D. I. Kondarides, *J. Catal.* **2004**, *225*, 327.

16 A. Basińskaa, T. P. Manieckib, W. K. Jóźwiakb, *React. Kinet. Catal. Lett.* **2006**, *89*, 319.

17 X. Wang, R. J. Gorte, J. P. Wagner, *J. Catal.* **2002**, *212*, 225.

18 H. Kušar, S. Hočevar, J. Levec, *Appl. Catal. B* **2006**, *63*, 194.

19 A. S. Quiney, Y. Schuurman, *Chem. Eng. Sci.* **2007**, *62*, 5026.

20 J. B. Ko, C. M. Bae, Y. S. Jung, D. H. Kim, *Catal. Lett.* **2005**, *105*, 157.

21 D. C. Grenoble, M. M. Estadt, D. F. Ollis, *J. Catal.* **1981**, *67*, 90.

22 P. Panagiotopoulou, D. I. Kondarides, *Catal. Today* **2006**, *112*, 49.

23 M. Krämer, M. Duisberg, K. Stoewe, W. F. Maier, *J. Catal.* **2007**, *251*, 410.

24 G. Germani, A. Stefanescu, Y. Schuurman, A. C. van Veen, *Chem. Eng. Sci.* **2007**, *62*, 5084.

25 G. Germani, P. Alphonse, M. Courty, Y. Schuurman, C. Mirodatos, *Catal. Today* **2005**, *110*, 114.

26 G. Germani, Y. Schuurman, *AIChE J.* **2006**, *52*, 1806.

27 W. TeGrotenhuis, K. Brooks, R. Dagle, J. Davis, J. Holladay, M. Kapadia, D. King, L. Pederson, B. Roberts, V. Stenkamp, *DOE Hydrogen Program, FY 2004 Progress Report*, **2004**.

28 A. S. Quiney, G. Germani, Y. Schuurman, *J. Power Sources* **2006**, *160*, 1163.

29 T. Baier, G. Kolb, *Chem. Eng. Sci.* **2007**, *62*, 4602.

30 O. Görke, P. Pfeifer, K. Schubert, *Appl. Catal. A* **2004**, *263*, 11.

31 E. V. Rebrov, S. A. Kuznetsov, M. H. J. M. de Croon, J. C. Schouten, *Catal. Today* **2007**, *125*, 88.

32 M. Pawlak, M. Thaler, V. Hacker, *Energy Fuels* **2007**, *21*, 2299.

33 G. Kolb, H. Pennemann, R. Zapf, *Catal. Today* **2005**, *110*, 121.

34 Y. Men, G. Kolb, R. Zapf, V. Hessel, H. Löwe, *Catal. Today* **2007**, *125*, 81.

35 O. Görke, P. Pfeifer, K. Schubert, *Catal. Today* **2005**, *110*, 132.